Electronic and structural properties of silicon carbide nanowires

R. Rurali
Laboratoire Collisions, Agrégats, Réactivité, IRSAMC, Université Paul Sabatier, 118 route de Narbonne, 31062 Toulouse cedex, France
(Received 26 January 2005; published 19 May 2005)

We present density-functional calculations of the geometrical and electronic structure of nanometer-thick silicon carbide nanowires grown along the ⟨100⟩ axis. We discuss first hydrogen-passivated wires and show that the quantum confinement results in a broadening of the band gap. Second, we study pure nanowires. In this case the facets' dangling bonds strongly reconstruct and the surface states that form turn the system into metallic. Both the gap broadening and the surface reconstruction driven metalization are analyzed in the case of C- and Si-rich wires.

DOI: 10.1103/PhysRevB.71.205405 PACS number(s): 73.22.−f, 81.07.Bc, 81.07.Lk

I. INTRODUCTION

In the latest years silicon carbide (SiC) has settled as one of the most interesting materials to replace silicon in high-power, high-frequency, and high-temperature device technology.[1,2] Its high breakdown field, high thermal conductivity, and high saturation velocity[3] concur in making SiC stand out from other wide band-gap materials (e.g., GaN, GaP, diamond), while having the benefit of a tractable materials technology, thanks to its superior chemical and mechanical stability and to the existence of a native oxide—silicon dioxide. So far, the most prominent bottleneck for an industrial-scale use of SiC has been the difficulty in obtaining high-quality large crystals. However, present progresses in single crystal growth[4] envisage the possibility to overcome these limitations, going toward a feasible SiC technology for the next-generation electronic devices capable of supplanting silicon in power electronics and harsh environment applications.

More recently, SiC has started to attract attention also as a material for nanotechnology applications. Cicero *et al.*[5] demonstrated the use of the alternation of C- and Si-terminated surfaces as a biocompatible, patterned substrate to control water interaction. Derycke *et al.*[6] reported the metalization of the Si-rich SiC(100) surface[7] by means of atomically controlled hydrogen adsorption,[6,8] which opens the way to the development of ohmic contacts on top of a chemically passive wide band-gap material. Zhang *et al.*[9] reported the emission of visible photoluminescence in 3C-SiC nanowhiskers, with applications in the field of light-emitting diodes, while the field electron emission properties of bunches of SiC needles have been investigated by Wu *et al.*[10] More in general, the synthesis of SiC nanostructures, e.g., hollow nanospheres,[11] nanosprings,[12] or nanowire-based flowerlike structures,[13] as novel functional elements for nanoscience is becoming an active field of research.

One-dimensional nanostructures deserve special attention, as they are expected to play a crucial role as building blocks of future molecular electronics applications.[14,15] Silicon carbide nanowires (SiCNWs) have the considerable advantage over silicon nanowires (SiNWs) of a much higher electrical conductance and an excellent mechanical stability, making them extremely interesting as scanning probe microscope tips, for instance, or to realize reliable nanocontacts for operation in a harsh environment. Moreover, the biocompatibility of SiC (see Ref. 5) makes SiCNWs ideally suited as interfaces capable of efficiently bridging biological systems to nanoelectronics devices.

SiCNWs can be grown by means of reaction with carbon nanotubes. Dai *et al.*[16] used multi-wall carbon nanotubes in a vapor-solid reaction, yielding SiCNWs—and other carbide nanorods—with diameters ranging from 2 to 30 nm. Zhang *et al.*[17] used single-wall nanotubes (SWNTs) in a solid-solid reaction, achieving a control of the growth process that allowed them to fabricate SWNT-SiCNW heterostructures with well-defined crystalline interface and with Schottky barrier-like *I-V* characteristic. SiCNWs can also be grown by chemical vapor deposition (CVD) and wires of 10 to 30 nm have been reported;[18,19] Zhou *et al.*[20] managed to reduce the nanowire size down to 5 nm using an iron particle as the catalyzer. Synthesis of SiCNWs by arc-discharge[21,22] or by direct chemical reaction[23] down to 10 nm have also been demonstrated. More recently, Yang *et al.*[24] proposed the synthesis of SiC nanorods by the thermal decomposition of a polymeric precursor with thicknesses ranging from 80 to 200 nm. A promising achievement for nanowire-based molecular electronics is the growth of coaxial SiCNWs, reported by Shen *et al.*[11]

Reducing the size pushes toward the approach of the *full quantum limit*, where the properties of the nanowire are substantially different from the bulk material. For this reason, a detailed knowledge of such systems is extremely interesting both from the fundamental physics standpoint and for what concerns the molecular electronics applications, because the device sizes are being continuously reduced and 10 nm thick SiCNWs can now be routinely grown.

In this paper we discuss on theoretical grounds the geometrical and electronic structure properties of nanometer-thick SiCNWs grown along the ⟨100⟩ direction with a bulk 3C-SiC core. We address explicitly the problem of surface reconstruction, comparing the results with analogous hydrogen passivated wires. The wires that we discuss are of the order of the thinnest SiCNWs grown so far[17,20] and can be viewed as a model for the diameter lower limit.

II. COMPUTATIONAL METHODS

In this work we present density-functional theory (DFT) calculations performed with the computer code SIESTA.[25,26] The core electrons have been represented by norm-conserving pseudopotentials of the Troullier-Martins type[27] in the Kleinman-Bylander separable form,[28] with core radii of 1.25 bohr for C and H and 1.90 bohr for Si. We have used a double-ζ basis set plus polarization functions[29] for the valence electrons and the generalized gradients approximation (GGA) due to Perdew, Burke, and Ernzerhof[30] for the exchange-correlation functional. The basis functions have been optimized following Anglada *et al.*[31] The numerical integrals have been performed on a grid fine enough to represent plane waves up to 100 Ry. The atomic positions have been relaxed using a conjugate gradient minimization algorithm until all the forces were reduced below 0.04 eV/Å. The Brillouin zone has been sampled with a highly converged set of k-points, using grids up to $(1\times1\times12)$ points according to the Monkhorst-Pack scheme.[32]

We have studied supercells of 57 and 114 atoms for the surface reconstructed SiCNWs and of 93 atoms for the hydrogen passivated SiCNWs (see below). The periodicity along the wire hampers the number of possible reconstructions, preventing from forming those that are not commensurable with the cell size. For this reason, we have also used a nonorthogonal tight-binding model[33,34] to explore larger cell sizes, up to 228-atom supercell, i.e., four unit cells of the wire. The tight-binding model employed proved to be extremely reliable in describing the nanoscale structural features of several systems[35–37] and gave a very good agreement with DFT in a previous study of silicon nanowires.[38] The survey carried out allowed us to conclude that no reconstruction with an extent larger than the unit cell is observed. This result is extremely robust, because it is not a question of the accuracy that tight-binding has in reproducing a bond length or a bond angle, but whether a reconstruction is found or not. All the geometries have been subsequently relaxed with DFT, but tight-binding permitted us to check that larger cells did not favor long-range reconstructions.

Convincing experimental evidence has shown that SiCNWs grow around a monocrystalline bulk core.[9,13,18–24] Unlike the case of Li *et al.*,[21] who reported 6H-SiC wires, in all the other cases the grown polytype was 3C-SiC (cubic or β-SiC), which is the one that we have chosen for this study. It should also be stressed that no polytype coexistence, i.e., polytype conversion along the wire's axis, has been reported so far.

Even though we have restricted our study to $\langle100\rangle$ SiCNWs, different wires' sections can be considered.[39] Generally, at the macroscopic scale the favored section can be deduced following the so-called Wulff's rule.[40,41] However, it has been shown that when the energy of the edges is no longer negligible, a situation that is common in the case of one-dimensional structure at the nanoscale, Wulff's rule breaks down.[39,41] In this work we study wires with rounded angles in a Wulff-like fashion,[38,40] because this is the only geometry that allows us to have all-C and all-Si facets, whose electronic structure analysis is one of the main purposes of this study (see below). However, the stability of other different sectioning arrangements cannot be discarded and merit a separate study.

III. HYDROGEN-PASSIVATED WIRES

The one-dimensionality of nanowires is known to induce a gap broadening as a result of the quantum confinement. In the case of silicon nanowires this has been reported by several authors (see, for instance, Refs. 42 and 43). For this to occur, it is necessary that no new surface state forms, in such a way that the nanowire can be viewed as a purely 1D-confined *bulk* system. This task is normally accomplished terminating the wire's dangling bonds with hydrogen. H-passivation prevents the surface from reconstructing, saturating its dangling bonds, and protects it against chemical attack, e.g., oxidation. The first part of this work has thus consisted in analyzing the nature of such an effect in the case of $\langle100\rangle$ SiCNWs.

Given the growth orientation and the geometry of the section, two kinds of SiCNWs coexist: in one case the most external layer is made of carbon atoms, while in the other it is made of silicon atoms. In bulk 3C-SiC—and in all the other SiC polytypes—one can change all Si atoms for C and vice versa without affecting the symmetry of the lattice and thus the properties of the material. Whenever the 3D bulk symmetry is broken this is no longer true, like in the SiC(100) surfaces, which are carbon *or* silicon terminated, and where, obviously, there is no symmetry with respect to the chemical species exchange. Throughout the rest of the paper we will call these two kinds of SiCNWs *carbon-coated* and *silicon-coated* wires, referring respectively to the C-rich and Si-rich phase.

We have analyzed the effect of H-termination in both the cases. In Fig. 1 we show the electronic density of states (DOS), comparing it with that of bulk 3C-SiC. It can be seen that both in the case of carbon-coated and silicon-coated SiCNWs, H-passivation results in a gap broadening, as expected. This is nothing more than the mentioned quantum confinement effect: the loss of two of the three dimensions of periodicity (with respect to the bulk) induces a discretization of the continuum of the electronic states, thus resulting in a broadening of the gap. The effect is especially evident in the case of the carbon-coated SiCNW where the band gap is approximately twice as large as the bulk case. Experimental evidence of quantum confinement has been recently reported in 3C-SiC nanocrystallites.[44]

The gap broadening is thus a pure effect of the confinement and hydrogen passivation intends to be a simple and effective model of all those experimental cases in which the formation of new surface states is prevented, e.g., oxidation,[18] and coverage with amorphous layers.[22]

The one-dimensional confinement is also expected to imply a loss of cohesion, at least at a certain degree. We have calculated the cohesion energies[45] of these wires, defined as

$$E_{coh} = -\left(E_{tot} - \sum_i n_i E_i\right), \tag{1}$$

where n_i is the number of atoms belonging to a given species and E_i is the corresponding energy for the isolated atom; the

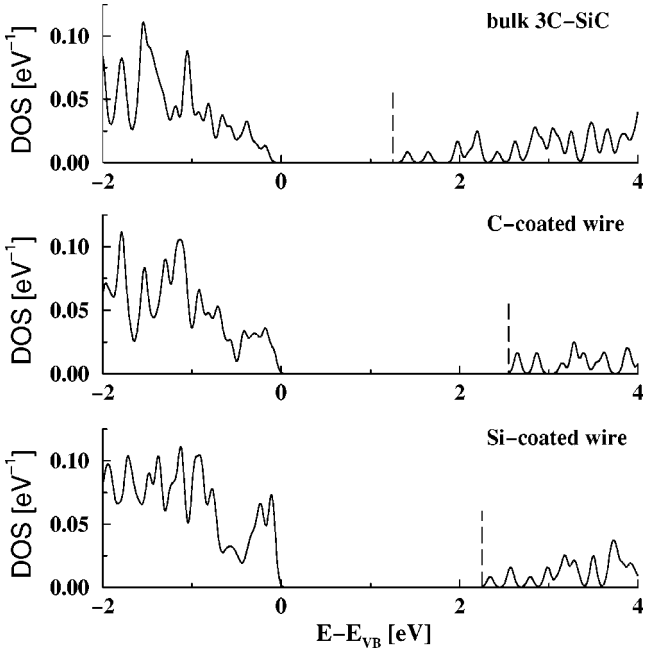

FIG. 1. The electronic density of states (DOS) of (a) bulk 3C-SiC, (b) carbon-coated SiCNW, and (c) silicon-coated SiCNW. The DOS plots have been normalized to the number of states in order to allow a comparison between systems calculated with different simulation cells and aligned to the top of the valence band. We have not compensated for the underestimation of the band gap, however the broadening-narrowing trend is expected to be correct.

sum runs over the species present in the system. We have obtained a cohesion energy of 4.66 eV/atom for C-coated wire and of 4.36 eV/atom for the Si-coated, compared to 6.32 eV/atom which is the value for bulk 3C-SiC. Despite a decrease of around 25%, the values obtained are still typical of well-bonded systems, e.g., of the same order of bulk silicon.

IV. SURFACE RECONSTRUCTED WIRES

A. Structural and mechanical properties

If the dangling bonds of the facets, i.e., the wire's lateral surface, are not passivated, their high reactivity makes them unstable and a reconstruction is expected to be favored, like it does in conventional infinite semiconducting surfaces.[46,47] We have considered the case of pure SiCNWs, the facets relaxation, and the corresponding electronic structure. A cross-section view of the minimum energy geometries found for the C- and Si-coated SiCNWs is shown in Fig. 2. In both the phases, the facet dangling bonds form rows of dimers, following the typical pattern of the infinite C(100) and Si(100) surfaces.[46,47] C dimers are much shorter than Si dimers, 1.39 Å against 2.59 Å, and form indistinctly on the {100} and on the {110} facets, while the rows of Si dimers are uniquely located at the {100} facets.

A major difference between the two phases is that the C atoms that dimerize favor an sp^2 rehybridization of their orbitals, resulting in an almost plain geometry, with bond angles of ~115°, that gives rise to an inward *shrinking* of the

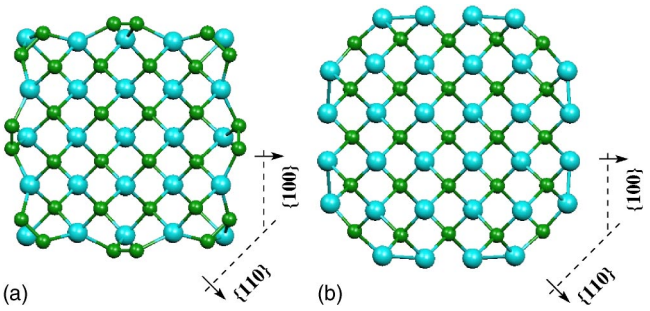

FIG. 2. (Color online) The cross-section view of the minimum energy geometry of (a) carbon-coated and (b) silicon-coated SiCNW.

dimers [see Figs. 2(a) and 3(a)]. The Si dimers of the Si-coated wire, on the other hand, narrow the bulk angle up to values of ~102–107°, allowing a slight outward protrusion with respect to the unrelaxed bulk terminated position [see Figs. 2(b) and 3(b)]. The different leveling of the dimer angles results also in a different effective *coverage* of the {100} facets, as it is shown in Fig. 4. The short C dimers of Fig. 4(a) are plain and tend to *enter* inside the facet, mixing with the inner Si shell. On the contrary, the Si dimers of Fig. 4(b) relax outward the facets, generating a thick all-Si outer layer. At variance with the {100} facets of silicon nanowires,[38] here the asymmetry of the dimers is almost negligible, though systematic. The formation of a *trough* in the center of the facet—which strictly speaking still takes place [see Fig. 4(b)]—is thus frustrated. We ascribe this difference to the higher rigidity of the C-Si bond with respect to the Si-Si bond. It is noteworthy that, contrary to the case of silicon nanowires, we have not found any other longer-range, competing reconstruction. In that case, we found that flipping one of every four dimers on the facet could give rise to a stable geometry.[38]

Welland *et al.*[13] reported the growth of SiCNWs covered with an outer graphite layer, while Seeger *et al.*[22] observed an amorphous-carbon coverage. Despite those wires being thicker than those considered in this study, that might be an indication of the existence of different C-rich phases and that further studies in this direction are needed. Still, it is remarkable that the *graphitization* trend of the surface, i.e., the sp^2 rehybridization, is captured even by the most simple C-rich structure.

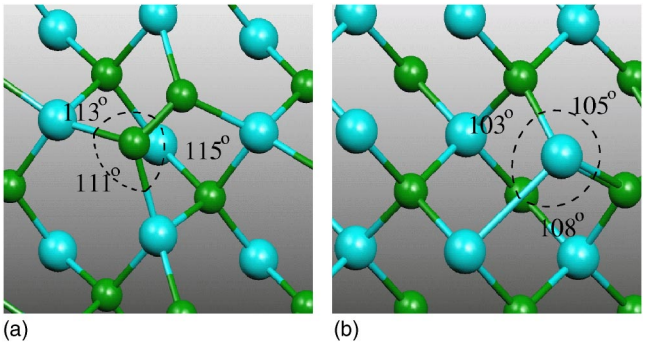

FIG. 3. (Color online) The detail of {100} facets: (a) symmetric C dimer of a C-coated wire and (b) asymmetric Si dimer of a Si-coated wire. The angles formed are indicated.

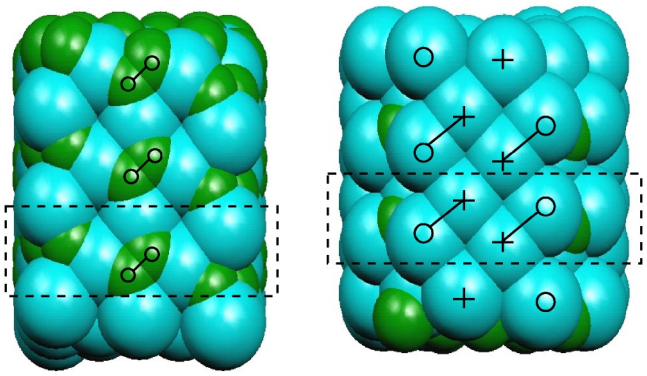

FIG. 4. (Color online) The minimum energy reconstruction of the {110} facet for (a) the carbon-coated and (b) the silicon-coated SiCNW. The Si dimers formed in the Si-coated are slightly asymmetric, as indicated, where crosses and balls refer to *inner* and *outer* atoms, respectively. The C dimers formed in the case C-coated wires [panel (a)], on the other hand, are symmetric.

One of the properties that makes SiC a more appealing choice in a variety of applications is its mechanical stability and its hardness. Such features could represent an important differential factor also for what concerns molecular electronics applications, i.e., if the wires are to be used as switches or contacts. To study the mechanical rigidity of the surface-reconstructed SiCNWs, we have calculated the Young's modulus, which accounts for the response to axial stress, according to

$$Y = \frac{1}{V_0}\frac{\partial^2 E}{\partial \epsilon^2}\bigg|_{\epsilon=0}, \tag{2}$$

where ϵ is the axial strain, and V_0 and E are the equilibrium volume and the total energy, respectively. We have obtained values of $\sim 255-280$ GPa. Therefore, $\langle 100 \rangle$ SiCNWs are approximately twice as rigid as SiNWs grown along the same direction, confirming the rigidity mismatch that holds in the bulk phase.[48] Despite the result being physically sound, this test is only apparently redundant. For what concerns thermal transport, for instance, recently Mingo and Broido[49] showed that a material with higher thermal conductivity is not necessarily the best nanowire thermal conductor. Hence, crossovers between the bulk and the nanowire properties cannot be discarded.

No qualitative change is detected in the cohesion energies [see Eq. (1)], which are 3.35 and 3.32 eV/atom for the C- and Si-coated SiCNW, respectively.

B. Electronic structure properties

The strong reconstruction the facets go through is expected to alter significantly the electronic structure of the whole wire. A band structure diagram is shown in Figs. 5 and 6 for both the C- and Si-coated SiCNW, respectively. Interestingly enough, it can be seen that the surface states due to the reconstruction cross the Fermi energy, thus indicating an induced metalization of the otherwise semiconducting wires. The C-coated wire has four states crossing the Fermi level (which are degenerate two by two). The Si-coated SiCNW, on the other hand, has five metallic states (two of which are degenerate), thus amounting to a maximum of five quanta of conductance. This is a remarkable result because it implies that nanometric-thick SiCNWs are conducting without the need of doping. The metalization relies on the reconstruction of the facets. Therefore, *confining* into the finite dimensions of a facet the corresponding infinite surface [C- or Si-terminated SiC (100)] alters the packing density of the surface layers, turning its electronic structure into metallic.

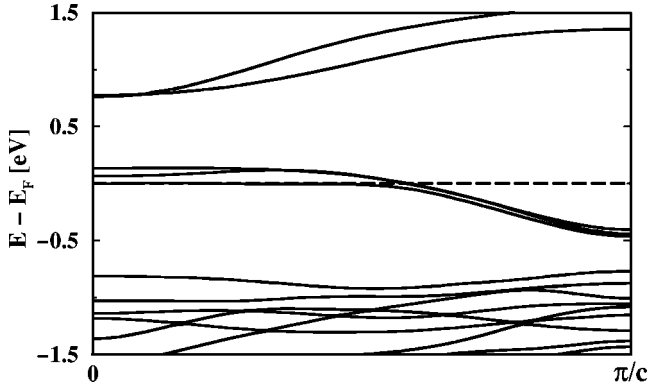

FIG. 5. The band structure of the C-coated SiCNW. Four states (two of which degenerate) cross the Fermi level at the center of the Brillouin zone.

The ability to control the doping concentration within certain tolerances is essential in the fabrication of standardized devices and it becomes a very critical task at the nanoscale. A rather high concentration of dopants in bulk SiC, e.g., $\sim 10^{19}$ cm^{-3}, amounts to having one dopant atom every $\sim$4480 C-Si pairs. In SiCNWs like those studied in this work, this would imply having one dopant atom every $\sim$70 nm of wire. Several authors reported doping concentrations of this order of magnitude in SiNW-based devices. However, it is clear that such a parameter becomes increasingly difficult to control and to reproduce reliably as the scale is reduced. In the case of thin nanowires, a statistical fluctuation of the doping concentration may imply to have no dopant at all in large regions of the system. For these reasons, the possibility to have conducting SiNWs (see Ref. 38) and SiCNWs without the need of doping should be properly considered.

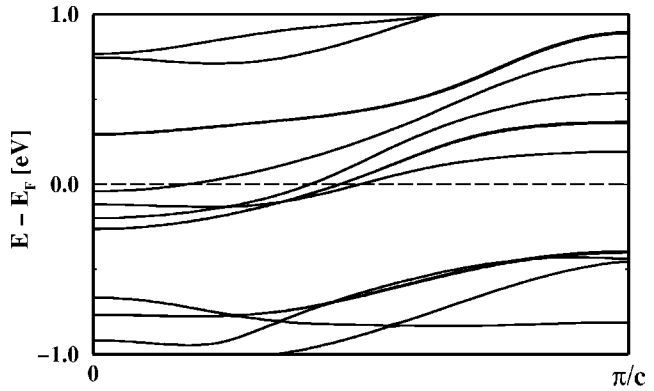

FIG. 6. The band structure of the Si-coated SiCNW. Five states (two of which degenerate) cross the Fermi level at different values of the wave vector k in the first half of the Brillouin zone.

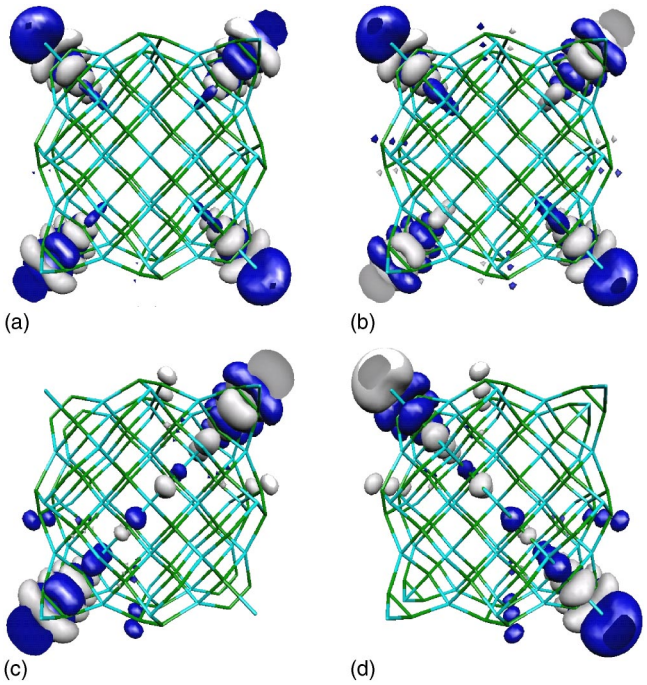

FIG. 7. (Color online) The wave function iso-surfaces of the four states of the C-coated SiCNW that cross the Fermi level (see Fig. 5). The degeneracy by pairs is revealed by the wave function symmetry.

The surface nature of the metallic states is evident in Figs. 7 and 8 where the representation in real space of the corresponding wave functions is shown. As can be seen there, the conduction will be sustained by the outer layers of the wires, with an almost negligible penetration in the bulk core.

It is well known that DFT underestimates the band gap in semiconductors and insulators. In this case, for instance, we have obtained 1.58 eV for bulk 3C-SiC [Fig. 1(a)] against the experimental value of ~2.2 eV. Therefore, one should take into account the possibility that the surface states arising inside the band gap are rather an artifact of the computational model. Despite the underestimation of the gap width, DFT is known to reproduce extremely well the dispersion of the bands, so that all the major technique for gap-error compensation consist in acting with a scissor operator on the band structure, rigidly shifting some of the states upward. Looking at Fig. 6 one notices that, operating on the five states that cross the Fermi level, it is not possible to open a gap without violating electron counting. Therefore the metalicity of the Si-coated wires seems to be robust against possible failure of DFT. Such an argument cannot be directly extended to the band structure of Fig. 5, where the four metallic states are degenerate by pairs and it cannot be excluded *a priori* that two of them should be shifted upward, opening a gap. Thus, the limitations of DFT only allow us to claim that the C-coated wire is semi-metallic or a small gap semiconductor.

An important difference between the C- and the Si-coated SiCNWs discussed is that, in the case of the latter, the metallic states cross the Fermi level at different k points. This increases the robustness of the metallic character of the wire, as it makes it unlikely that a gap opened due to Peierls distortion destroys the metalicity. On the contrary, this is possible in the case of the C-coated SiCNW, where all the metallic states cross the Fermi level at the same wave vector k.

V. CONCLUSIONS

We have studied nanometer-thick SiCNWs with density-functional calculations. When the dangling bonds of the facets are terminated with hydrogen, the formation of surface states is prevented and SiCNWs are semiconducting. The gap is broadened as an effect of quantum confinement, both

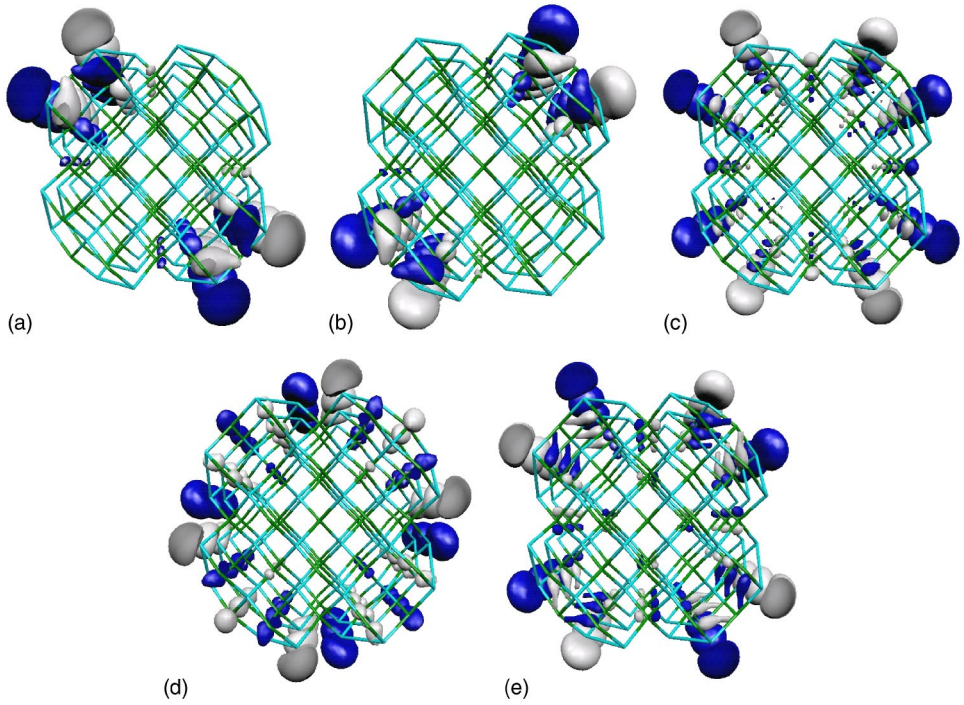

FIG. 8. (Color online) The wave function iso-surfaces of the five states of the Si-coated SiCNW that cross the Fermi level (see Fig. 6). The degeneracy of states (a) and (b) can be appreciated.

in the case of C- and Si-rich wires. In the absence of such a passivation the facets strongly reconstruct in search for an energetically stable configuration. This rearrangement of the facets' atoms results in a metalization of the wire. The metallic states are surface states, thus the conduction is sustained almost entirely by the outer layers of the wire.

Both the gap-broadening of the H-passivated wires and the metalization of the surface reconstructed wires are expected to depend on the diameter thickness. In the limit of very large diameter the quantum confinement will not play any role and the electronic features of the {100} facets will approach that of the corresponding infinite (100) surfaces, which are both semiconducting. However, even though the dependence of the gap-broadening of passivated SiCNWs on the diameter is expected to be monotonic, it is more difficult to figure out when the metalicity of the surface reconstructed wires breaks down. A detailed analysis of the dependence of the electronic properties of SiCNWs on the size is thus required to improve the understanding of these systems.

ACKNOWLEDGMENTS

This work has been financially supported by the Generalitat de Catalunya, through the NANOTEC program. E. Anglada is greatly acknowledged for his help in optimizing the basis set used in the calculation. Thanks to N. Lorente and N. Mestres for the useful suggestions concerning the writing of the manuscript.

[1] R. Madar, Nature (London) **430**, 974 (2004).
[2] P. Deák, Mater. Sci. Forum **430**, 974 (2004).
[3] *Recent Major Advances in SiC*, edited by W. J. Choyke, H. Matsunami, and G. Pensl (Springer, Berlin, 2004).
[4] D. Nakamura, I. Gunjishima, S. Yamaguchi, T. Ito, A. Okamoto, H. Kondo, S. Onda, and K. Takatori, Nature (London) **430**, 1009 (2004).
[5] G. Cicero, A. Catellani, and G. Galli, Phys. Rev. Lett. **93**, 016102 (2004).
[6] V. Derycke, P. Soukiassian, F. Amy, Y. J. Chabal, M. D'Angelo, H. B. Enriquez, and M. G. Silly, Nat. Mater. **2**, 253 (2003).
[7] F. Amy and Y. J. Chabal, J. Chem. Phys. **119**, 6201 (2003).
[8] R. Rurali, E. Wachovicz, P. Ordejón, and P. Hyldgaard (unpublished).
[9] Y. Zhang, M. Nishitani-Gamo, C. Xiao, and T. Ando, J. Appl. Phys. **91**, 6066 (2002).
[10] Z. S. Wu, S. Z. Deng, N. S. Xu, J. Chen, J. Zhou, and J. Chen, Appl. Phys. Lett. **80**, 3829 (2002).
[11] G. Shen, D. Chen, K. Tang, Y. Qian, and S. Zhang, Chem. Phys. Lett. **375**, 177 (2003).
[12] D. Zhang, A. Alkhateeb, H. Han, H. Mahmood, D. N. McIllroy, and M. Grant Norton, Nano Lett. **3**, 983 (2003).
[13] G. W. Ho, A. S. W. Wong, D. J. Kang, and M. E. Welland, Nanotechnology **15**, 996 (2004).
[14] D. Appell, Nature (London) **419**, 553 (2002).
[15] C. M. Lieber, Nano Lett. **2**, 81 (2002).
[16] H. Dai, E. W. Wong, Y. Z. Lu, S. Fan, and C. M. Lieber, Nature (London) **375**, 769 (1995).
[17] Y. Zhang, T. Ichihashi, C. Landree, F. Nihey, and S. Iijima, Science **285**, 1719 (1999).
[18] C. Liang, G. Meng, L. Zhang, Y. Wu, and Z. Cui, Chem. Phys. Lett. **329**, 323 (2000).
[19] G. Meng, L. Zhang, C. Mo, S. Zhang, Y. Qin, S. Feng, and H. Li, Solid State Commun. **106**, 215 (1998).
[20] X. Zhou, H. Lai, H. Peng, C. F. C. K. Au, L. Liao, N. Wang, I. Bello, C. Lee, and S. Lee, Chem. Phys. Lett. **318**, 58 (2000).
[21] Y. Li, S. Xie, W. Zhou, L. Ci, and Y. Bando, Chem. Phys. Lett. **356**, 325 (2000).
[22] T. Seeger, P. Redlich, and M. Rühle, Adv. Mater. (Weinheim, Ger.) **12**, 279 (2000).
[23] Q. Lu, J. Hu, K. Tang, and Y. Qian, Appl. Phys. Lett. **75**, 507 (1999).
[24] W. Yang, H. Miao, Z. Xie, L. Zhang, and L. An, Chem. Phys. Lett. **383**, 441 (2004).
[25] P. Ordejón, E. Artacho, and J. M. Soler, Phys. Rev. B **53**, R10 441 (1996).
[26] J. Soler, E. Artacho, J. D. Gale, A. García, J. Junquera, P. Ordejón, and D. Sánchez-Portal, J. Phys.: Condens. Matter **14**, 2745 (2002).
[27] N. Troullier and J. L. Martins, Phys. Rev. B **43**, 1993 (1991).
[28] L. Kleinman and D. M. Bylander, Phys. Rev. Lett. **48**, 1425 (1982).
[29] E. Artacho, D. Sánchez-Portal, P. Ordejón, A. García, and J. M. Soler, Phys. Status Solidi B **215**, 809 (1999).
[30] J. P. Perdew, K. Burke, and M. Ernzerhof, Phys. Rev. Lett. **77**, 3865 (1996).
[31] E. Anglada, J. M. Soler, J. Junquera, and E. Artacho, Phys. Rev. B **66**, 205101 (2002).
[32] H. J. Monkhorst and J. D. Pack, Phys. Rev. B **8**, 5747 (1973).
[33] D. Porezag, T. Frauenheim, T. Köhler, G. Seifert, and R. Kaschner, Phys. Rev. B **51**, 12 947 (1995).
[34] R. Rurali and E. Hernández, Comput. Mater. Sci. **28**, 85 (2003).
[35] E. Hernández, C. Goze, P. Bernier, and A. Rubio, Phys. Rev. Lett. **80**, 4502 (1998).
[36] Y. Zhao, B. I. Yakobson, and R. E. Smalley, Phys. Rev. Lett. **88**, 185501 (2002).
[37] E. Hernández, V. Meunier, B. W. Smith, R. Rurali, H. Terrones, M. Buongiorno Nardelli, M. Terrones, D. E. Luzzi, and J.-C. Charlier, Nano Lett. **3**, 1037 (2003).
[38] R. Rurali and N. Lorente, Phys. Rev. Lett. **94**, 026805 (2005).
[39] R. Rurali and N. Lorente, Nanotechnology **16**, S250 (2005).
[40] S. Ismail-Beigi and T. Arias, Phys. Rev. B **57**, 11 923 (1998).
[41] Y. Zhao and B. I. Yakobson, Phys. Rev. Lett. **91**, 035501 (2003).
[42] B. Delley and E. F. Steigmeier, Appl. Phys. Lett. **67**, 2370 (1995).
[43] X. Zhao, C. M. Wei, L. Yang, and M. Y. Chou, Phys. Rev. Lett. **92**, 236805 (2004).
[44] X. L. Wu, J. Y. Fan, T. Qiu, X. Yang, G. G. Siu, and P. K. Chu, Phys. Rev. Lett. **94**, 026102 (2005).
[45] A more rigorous definition of the cohesion energy requires us to take into account also the zero-point vibrational energy that is obtained by simply integrating the vibrational density of states

[see for instance K. J. Chang and M. L. Cohen, Phys. Rev. B **35**, 8196 (1987)]. Calculating a full phonon spectrum of the SiC-NWs that we study here is beyond the scope of this work. For this reason, in order to provide comparisons on equal footing, neither have we considered the zero-point energy for the calculation of the cohesion energy of bulk system that we give as reference.

[46] D. R. Alfonso, D. A. Drabold, and S. E. Ulloa, Phys. Rev. B **51**, 14 669 (1995).

[47] D. J. Chadi, Phys. Rev. Lett. **43**, 43 (1979).

[48] We estimated a value of 167 GPa with tight-binding calculation for ⟨100⟩ silicon nanowires (see Ref. 38).

[49] N. Mingo and D. A. Broido, Phys. Rev. Lett. **93**, 246106 (2004).